Atmos. Chem. Phys. Discuss., https://doi.org/10.5194/acp-2019-123
Manuscript under review for journal Atmos. Chem. Phys.
Discussion started: 12 March 2019

Atmospheric Chemistry and Physics Discussions

Exploiting multi-wavelength aerosol absorption coefficients in a multi-time source apportionment study to retrieve source-dependent absorption parameters

Alice C. Forello[1], Vera Bernardoni[1], Giulia Calzolai[2], Franco Lucarelli[2], Dario Massabò[3], Silvia Nava[2], Rosaria E. Pileci[1,a], Paolo Prati[3], Sara Valentini[1], Gianluigi Valli[1], Roberta Vecchi[1]

[1]Department of Physics, Università degli Studi di Milano and National Institute of Nuclear Physics INFN-Milan, via Celoria 16, Milan, 20133, Italy

[2]Department of Physics and Astronomy, Università di Firenze and National Institute of Nuclear Physics INFN-Florence, via G. Sansone 1, Sesto Fiorentino, 50019, Italy

[3]Department of Physics, Università degli Studi di Genova and National Institute of Nuclear Physics INFN- Genoa, via Dodecaneso 33, Genoa, 16146, Italy

[a]now at: Laboratory of Atmospheric Chemistry (LAC), Paul Scherrer Institut (PSI), Forschungsstrasse 111, Villigen, 5232, Switzerland

Correspondence to: Roberta Vecchi (roberta.vecchi@unimi.it)

Abstract. In this paper, a new methodology coupling aerosol optical and chemical parameters in the same source apportionment study is reported. This approach gives additional relevant information such as estimates for the atmospheric Ångström Absorption Exponent (α) of the sources and Mass Absorption Coefficient (MAC) for fossil fuel emissions at different wavelengths.

A multi-time source apportionment study using Multilinear Engine ME-2 was performed on a PM10 dataset with different time resolution (24 hours, 12 hours, and 1 hour) collected during two different seasons in Milan (Italy) in 2016. Samples were optically analysed to retrieve the aerosol absorption coefficient b_{ap} (in Mm^{-1}) at four wavelengths (λ=405 nm, 532 nm, 635 nm and 780 nm) and chemically characterised for elements, ions, levoglucosan, and carbonaceous components. Time-resolved chemically speciated data were coupled with b_{ap} multi-wavelength measurements and introduced as input data in the multi-time receptor model; this approach was proven to strengthen the identification of sources being particularly useful when important chemical markers (e.g. levoglucosan, elemental carbon, …) are not available. The

final solution consisted in 8 factors (nitrate, sulphate, resuspended dust, biomass burning, construction works, traffic, industry, aged sea salt); the implemented constraints led to a better physical description of factors and the bootstrap analysis supported the goodness of the solution. As for b_{ap} apportionment, consistently to what expected, the two factors assigned to biomass burning and traffic were the main contributors to aerosol absorption in atmosphere. A relevant feature of the approach proposed in this work is the possibility of retrieving many other information about optical parameters; for example, opposite to the more traditional approach used by optical source apportionment models, here we obtained the atmospheric Ångström Absorption Exponent (α) of the sources (α biomass burning = 1.83 and α fossil fuels = 0.80), without any a priori assumption. In addition, an estimate for the Mass Absorption Cross section (MAC) for fossil fuel emissions at four wavelengths was obtained and found to be consistent with literature ranges.

1. Introduction

Atmospheric aerosol impacts both on local and global scale causing adverse health effects (Pope and Dockery, 2006), decreasing visibility (Watson, 2002) and influencing the climate (IPCC, 2013). To face these issues an accurate knowledge of the aerosol emission sources is mandatory.

At the state of the art, multivariate receptor models are considered a robust approach (Belis et al., 2015) to carry out source apportionment studies of atmospheric aerosol and the Positive Matrix Factorization (PMF) (Paatero and Tapper, 1994) has become one of the most widely used receptor models (Hopke, 2016). In the late 1990s the Multilinear Engine (ME2) was implemented, a very flexible algorithm to solve multilinear and quasi-multilinear problems (Paatero, 1999). This algorithm introduced the possibility to write scripts and implement advanced receptor modelling approaches; one example is the multi-time model, developed for the first time by Zhou et al. (2004), which uses each experimental data in its original time schedule as model input. This approach is very useful in measurement campaigns when instrumentation with different time resolution (minutes, hours or days) is available; indeed, with the multi-time approach, high time resolution data can be exploited without averaging them over the longest sampling interval. Nevertheless, source apportionment studies carried out by multi-time model are still scarce in the literature (Zhou et al., 2004; Ogulei et al., 2005; Kuo et al., 2014; Liao et al., 2015; Crespi et al., 2016; Sofowote et al., 2018).

The combination of time-resolved chemically speciated data with the information obtained from instrumentation measuring aerosol optical properties at different wavelengths (e.g. the absorption coefficient b_{ap}) is suggested as one of the future investigations of receptor modelling (Hopke, 2016); however, to the best of our knowledge, very few attempts in this direction have been done (recently e.g. Xie et al., 2019). Wang et al. (2011, 2012) introduced in a source apportionment study the Delta-C (Delta-C = BC@370 nm – BC@880 nm from aethalometer measurements) as an input

variable in a source apportionment study and found that Delta-C was very useful in separating traffic from wood burning source contributions.

The wavelength dependence of b_{ap} can be empirically considered proportional to $\lambda^{-\alpha}$, where α is the Ångström Absorption Exponent; α depends on particles composition and size, and it is a useful parameter to gain information about particles type in atmosphere (see e.g. Yang et al., 2009). Among PM components, black carbon (BC) is the main responsible for light absorption in atmosphere; in fact, it is considered the main PM contributor to global warming and the second most important anthropogenic contributor after CO_2 (Bond et al., 2013). Black carbon refers to a fraction of the carbonaceous aerosol that shares peculiar features about microstructure, morphology, thermal stability, solubility, and light absorption (Petzold et al., 2013); in particular, it is characterised by a wavelength-independent imaginary part of the refractive index over visible and near-visible regions. In the last decade, experimental studies evidenced also the role of another absorbing component i.e. brown carbon (BrC), referred to as light-absorbing organic matter of various origins with increasing absorption towards lower wavelengths, especially in the UV region (Andreae and Gelencsér, 2006). BrC is an aerosol component that also affects the elemental vs. organic carbon correct separation when using thermal-optical methods as recently outlined by Massabò et al. (2016).

Source apportionment optical models based only on multi-wavelength measurements of b_{ap} are available in the literature, i.e. the widespread Aethalometer model (Sandradewi et al., 2008) and the more recent Multi-Wavelength Absorption Analyzer (MWAA) model (Massabò et al., 2015; Bernardoni et al., 2017b). Briefly, these models allow to estimate the contribution of sources to aerosol absorption in atmosphere exploiting their different dependence on λ (different α). As a step forward, MWAA provides the b_{ap} apportionment in relation to both the sources and the components (i.e. BC and BrC) and gives also an estimate for α of BrC. Source apportionment optical models usually assume two contributors to b_{ap}, namely fossil fuels combustion and wood burning (only few exceptions are present in the literature, e.g. Fialho et al., 2005). In most cases this assumption is well founded, except in presence of episodic events that give a not negligible contribution to aerosol absorption in atmosphere, such as the transport of mineral dust from the Saharan desert (Fuzzi et al., 2015). Moreover, the above-mentioned models need a priori assumption about α of the sources; this is the most critical step, since α depends on the kind of fuel, burning conditions and aging processes in the atmosphere and wide ranges for α are reported in literature (Sandradewi et al., 2008). Without accurate determination of source-specific atmospheric α (for example exploiting the information derived from source apportionment using ^{14}C measurements), the applicability of models based on optical determination is questionable (Bernardoni et al., 2017b; Massabò et al., 2015; Zotter et al., 2017). Moreover, the generally accepted assumption of α=1 for fossil fuels and BC, that is derived from the theory of absorption of spherical particles in the Rayleigh regime (Seinfeld and Pandis, 2006), might not always be valid in atmosphere due to aerosol aging processes (Liu et al., 2018).

In this work, in the frame of a source apportionment study based on multi-time receptor modelling, optical and chemical data were coupled to explore the possibility of retrieving a multi-λ apportionment of b_{ap} with no need of a-priori assumptions on the contributing sources. Opposite, with this approach source-dependent α values can be provided as output. Moreover, the multi-λ apportionment of b_{ap} in each source allowed to estimate MAC values at different wavelengths, exploiting the well-known relation $EBC=b_{ap}(\lambda)/MAC(\lambda)$ (Bond and Bergstrom, 2006) and considering the apportioned concentrations of elemental carbon (EC) as a proxy for BC. It is noteworthy that the evaluation of atmospheric MAC values is not trivial due to the possible presence of absorbing components different from BC (e.g. contribution from BrC, especially at lower wavelengths).

The original approach proposed in this work shows that coupling the chemical and optical information in a receptor modelling process is particularly advantageous because: (1) strengthens the source identification, that is particularly useful when relevant chemical tracers (e.g. levoglucosan, EC, …) are not available; (2) gives estimates for source-specific atmospheric Ångström Absorption Exponent (α) which are typically assumed a-priori in optical apportionment models; (3) assesses MAC values at different wavelengths for specific sources.

2. Material and methods

2.1 Site description and aerosol sampling

Two measurement campaigns were performed during summertime (June-July) and wintertime (November-December) 2016 in Milan (Italy). Milan is the largest city (more than 1 million inhabitants, doubled by commuters everyday) of the Po Valley, a very well-known hot-spot pollution area in Europe due to both large emissions from a variety of sources (i.e. traffic, industry, domestic heating, energy production plants, and agriculture) and low atmospheric dispersion conditions (e.g. Vecchi et al., 2007 and 2019; Perrone et al., 2012; Bigi and Ghermandi, 2014; Perrino et al., 2014).

The sampling site is representative of the urban background and it is situated at about 10 meters above the ground, on the roof of the Physics Department of the University of Milan, less than 4 km far from the city centre (Vecchi et al., 2009). It is important to note that during the sampling campaigns, a large building site was in activity next to the monitoring station.

Aerosol sampling was carried out using instrumentation with different time-resolution. Low time resolution PM10 data, with a sampling duration of 24 and 12 hours during summertime (20 June-22 July 2016) and wintertime (21 November-22 December 2016), respectively, were collected in parallel on PTFE (Whatman, 47 mm diameter) and pre-fired (700 °C, 1 hour) quartz-fibre (Pall, 2500QAO-UP, 47 mm diameter) filters. Low volume samplers with EPA PM10 inlet operating at 1 $m^3 h^{-1}$ were used. High time resolution data were collected during shorter periods (11 July-18 July and 21 November-28 November 2016) by a streaker sampler (D'Alessandro et al., 2003). Shortly, the streaker sampler collects the fine and

coarse PM fractions (particles with aerodynamic diameter $d_{ae} < 2.5$ µm, and $2.5 < d_{ae} < 10$ µm, respectively) with hourly resolution. Particles with $d_{ae} > 10$ µm impact on the first stage and are discarded; the coarse fraction deposits on the second stage, consisting of a Kapton foil; finally, the fine fraction is collected on a polycarbonate filter. The two collecting supports are kept in rotation with an angular speed of about 1.8° h^{-1} to produce a circular continuous deposit on both stages.

Meteorological data were available at a monitoring station belonging to the regional environmental agency (ARPA Lombardia) which is less than 1 km far away.

2.2 PM mass concentration and chemical characterisation

PM10 mass concentration was determined on PTFE filters by gravimetric technique. Weighing was performed by an analytical balance (Mettler, model UMT5, 1 µg sensitivity) after a 24 hours conditioning period in an air-controlled room as for temperature (20 ± 1 °C) and relative humidity (50 ± 3 %) (Vecchi et al., 2004).

These filters were then analysed by Energy Dispersive X-Ray Fluorescence (ED-XRF) analysis to obtain the elemental composition (details on the procedure can be found in Vecchi et al., 2004). For most elements and samples, concentrations were characterised by relative uncertainties in the range 7-20 % (higher uncertainties for elements with concentrations next to MDL) and Minimum Detection Limits (MDL) of 0.9-30 ng m^{-3} with the above mentioned sampling conditions.

Quartz-fibre filters were punched and analysed to detect levoglucosan, sulphate, nitrate, and carbonaceous components. For each filter, one punch (1.5 cm^2) was extracted by sonication (1 h) using 5 ml ultrapure Milli-Q water; this extract was analysed to measure both levoglucosan and inorganic anions concentrations. Levoglucosan concentration was determined by High-Performance Anion Exchange Chromatography coupled with Pulsed Amperometric Detection (HPAEC-PAD) (Piazzalunga et al., 2010) only in winter samples. Indeed, as already pointed out by other studies at the same sampling site (Bernardoni et al., 2011) and as routinely measured at monitoring stations in Milan by the Regional Environmental Agency (private communication), levoglucosan concentrations during summertime are lower than the MDL of the technique (about 6 ng m^{-3}), due to both lower emissions (no influence of residential heating and negligible impact from other sources) and higher OH levels in the atmosphere depleting molecular markers concentrations (Robinson et al., 2006; Hennigan et al., 2010). Uncertainties on levoglucosan concentration were about 11 %. The measurement of main water-soluble inorganic anions (SO_4^{2-} and NO_3^-) was performed by Ion Chromatography (IC) with MDL of 25 and 50 ng m^{-3} with summertime and wintertime sampling conditions, respectively, and uncertainties of about 10 %. Unfortunately, due to technical problems no data on ammonium were available. Details on the analytical procedure for IC analysis are reported in Piazzalunga et al. (2013). Another punch (1.0 cm^2) of each filter was analysed by Thermal Optical Transmittance analysis (TOT, Sunset Inc., NIOSH-870 protocol) (Piazzalunga et al., 2011) in order to assess organic and

elemental carbon (OC and EC) concentrations. MDL was 75 and 150 ng m^{-3} with summertime and wintertime sampling conditions, respectively, and uncertainties were about 10-15 %.

High time resolution samples were analysed to obtain the elemental composition by Particle Induced X-ray Emission (PIXE) technique, using a properly collimated proton beam and scanning the deposits in steps corresponding to 1-hour aerosol deposit (details in Calzolai et al., 2015). In this work, fine and coarse elemental concentrations determined by PIXE analysis were added up to obtain PM10 concentrations with hourly resolution as low time resolution PM10 samples were also available.

2.3 Aerosol light-absorption coefficient measurements

The aerosol absorption coefficient (b_{ap}) at the 4 wavelengths λ = 405, 532, 635 and 780 nm was measured on both low and high time resolution samples with the home-made polar photometer PP_UniMI (Vecchi et al., 2014; Bernardoni et al., 2017c). Low time resolution optical measurements were performed on PTFE filters since their physical characteristics can be considered more similar to polycarbonate filters used by the streaker sampler. Indeed, Vecchi et al. (2014) reported that aerosol absorption measurements on samples collected in parallel on quartz-fibre and PTFE filters showed significant differences, which were mainly ascribed to sampling artefacts due to organics affecting quartz-fibre filters. For high time resolution samples, b_{ap} was measured only in the fine fraction collected on polycarbonate filters, since absorption from the Kapton foil on which the coarse fraction was collected did not allow b_{ap} assessment. Anyway, b_{ap} values in PM2.5 and PM10 were expected to be fairly comparable, as most of the contribution to aerosol absorption in atmosphere is typically given by particles in the fine fraction at heavily polluted urban sites like Milan. To verify this assumption, high time resolution b_{ap} data in PM2.5 were averaged on the time scale of low time resolution b_{ap} in PM10 for comparison. They turned out to be in good agreement, between 11 % and 13 % depending on the λ, except for b_{ap} at λ=405 nm that showed a higher difference (27 %) but with most data (83 %) within experimental uncertainties. To take into account for this difference, b_{ap} data at λ=405 nm were homogenised before their insertion into the model, following the criterion used for chemical species (for further detail about homogenisation procedure, see Sect. 2.4 and Sect. 2.5).

Uncertainties on b_{ap} were about 15 %. MDL was in the range 1-10 Mm^{-1} depending on sampling duration and wavelength. Optical system stability was checked during the measurement session, evaluating the reproducibility of the measure of a blank test filter. Laser stability was also checked at least twice a day and the recorded intensities were used to normalise blank and sampled filters analysis.

2.4 Model description

Multivariate receptor models (Henry, 1997) represent one of the most widespread and robust approaches used to carry out source apportionment studies for atmospheric aerosol (Belis et al., 2014 and 2015). In particular, the Positive Matrix Factorization (Paatero and Tapper, 1994; Paatero, 1997) has been extensively used in the literature and, afterwards, the Multilinear Engine ME2 (Paatero, 1999 and 2000) introduced the possibility of solving all kinds of multilinear and quasi-multilinear problems. The fundamental principle is the mass conservation between the emission source and the receptor site: focusing on the aerosol properties at the receptor site (i.e. measuring a large number of chemical constituents in different samples), a mass balance analysis can be performed to identify the factors influencing aerosol concentrations (Hopke, 2016). Factors can be subsequently interpreted as the main sources impacting the site, exploiting the characterisation of the most relevant sources in the investigated area or the adoption of fingerprints available from previous literature works (Belis et al., 2014). Referring to the input data as matrix X (matrix elements x_{ij}), the chemical profile of the factors as matrix F (matrix elements f_{kj}), and the time contribution of the factors as matrix G (matrix elements g_{ik}), the main equation of a bilinear problem can be written as follows:

$$x_{ij} = \sum_{k=1}^{P} g_{ik} f_{kj} + e_{ij} \qquad (1)$$

where the indices i, j, and k indicate the sample, the species, and the factor, respectively; P is the number of factors and the matrix E (matrix elements e_{ij}) is composed by the residuals, i.e. the difference between measured and modelled values. In this way, a system of NxM equations is established, where N is the number of samples and M is the number of species. The solution of the problem is computed minimising the object function Q defined as:

$$Q = \sum_{i=1}^{N} \sum_{j=1}^{M} \left(\frac{e_{ij}}{\sigma_{ij}} \right)^2 \qquad (2)$$

where σ_{ij} are the uncertainties related to the input data.

The multi-time receptor model was developed in order to use each data value in its original time schedule, without averaging the high time resolution data or interpolating the low time resolution data (Zhou et al., 2004; Ogulei et al., 2005). The main Eq. (1) is consequently modified as below:

$$x_{sj} = \frac{1}{t_{s2} - t_{s1} + 1} \sum_{k=1}^{P} f_{kj} \sum_{i=t_{s1}}^{t_{s2}} g_{ik} \eta_{jm} + e_{sj} \qquad (3)$$

where the indices s, j, and k indicate the sample, the species and the factor respectively; P is the number of factors; t_{s1} and t_{s2} are the starting and ending time for the s-th sample in time units (i.e. the shortest sampling interval, that is 1 hour for the dataset of this work) and i represents one of the time units of the s-th sample. η_{jm} are adjustment factors for chemical species replicated with different time resolution and measured with different analytical methods (represented by the subscript m).

If η is close to unity, species concentration measured by different analytical approaches can be considered in good agreement; non-replicated species have adjustment factors set to unity by default. In this work, the adjustment factors were always set to unity in the model; to take into account the use of different aerosol samplers (i.e. low volume sampler with EPA inlet and streaker sampler) and different analytical techniques to obtain the elemental composition (i.e. ED-XRF and PIXE), concentrations of replicated species with different time resolution were homogenised before inserting them into the input matrix X, as will be explained in Sect. 2.5. Applying this data treatment procedure, it is possible to avoid the check of the consistency, from the experimental point of view, of the η values calculated by the model. Otherwise, this step should always be performed after running the model.

In the multi-time model a regularisation equation is introduced, since some sources could contain few or no species measured with high time resolution:

$$g_{(i+1)\,k} - g_{ik} = 0 + \varepsilon_i \qquad (4)$$

where ε_i represent the residuals.

As already pointed out in a previous work (Ogulei et al., 2005), a weighting parameter for low resolution species (24 or 12 hours in this work) might be necessary; in this study, it was implemented in the equations and set at 0.5 for strong species (not applied to weaker species as Na, Mg, and Cr, see Sect. 2.5).

Equations (3) and (4) were solved using the Multilinear Engine (ME) program (Paatero, 1999). In Eq. (2), the object function Q takes into account residuals from the main Eq. (3) and from the auxiliary equations (regularisation Eq. (4), normalisation equation, pulling equations, and constraints).

In this work, the multi-time model implemented by Crespi et al. (2016) is used. Using this model implementation, constraints can be inserted in the model and the bootstrap analysis is also performed to evaluate the robustness of the final solution.

2.5 Input data

As already mentioned in Sect. 2.4, instead of using adjustment factors in the model (all set equal to one), concentrations of replicated species with different time resolution were pre-homogenised and then inserted into the input matrix X. Concentration data with longer sampling interval (24 and 12 hours in this work) were considered as benchmark, since analytical techniques usually show a better accuracy on concentration values far from MDL (i.e. samples collected on longer time intervals) (Zhou et al., 2004; Ogulei et al., 2005).

Variables were then classified as weak and strong based on the signal to noise ratio (S/N) criterion (Paatero, 2015). For hourly data only strong variables (S/N ≥ 1.2) were considered; for low time resolution data also weaker variables as Na,

Mg and Cr (with S/N equal to about 0.8), that resulted strong variables in hourly samples, were also inserted (with uncertainties comparable to concentration values) in order to avoid the exclusion of too many data. Indeed, excluding these low time resolution variables from the analysis gave rise to artificial high values in the source time contribution matrix for those sources traced by these species (in this case it was particularly important for aged sea salt traced by Na and Mg, see Sect. 3.1); this oddity was already reported by Zhou et al. (2004).

Variables with more than 20 % of the concentration data below MDL values were omitted from the analysis (Ogulei et al., 2005). The procedure described in Polissar et al. (1998) was followed to treat uncertainties and below MDL data. In general, missing concentration values were estimated by linear interpolation of the measured data and their uncertainties were assumed as three times this estimated value (Zhou et al., 2004; Ogulei et al., 2005). As for summertime levoglucosan data (not available), the approach was to include them as below MDL data and not as missing data following Zhou et al. (2004), who underlined that the multi-time model is more sensitive to missing values than the original PMF model. In order to avoid double counting, in this study S was chosen as input variable instead of SO_4^{2-} as it was determined on both low time- and high time-resolution samples (by XRF and PIXE analysis, respectively, see Calzolai et al., 2008). However, elemental SO_4^{2-} and S concentrations showed a high correlation (correlation coefficient R=0.98) and the Deming regression gave a slope of 2.69 ± 0.13 (sulphate vs. sulphur) with an intercept of -198 ± 82, i.e. compatible with zero within 3 standard deviations. The slight difference (of the order of 10%) between the estimated slope and the SO_4^{2-}-to-S stoichiometric coefficient (i.e. 3) can be ascribed to either a small fraction of insoluble sulphate or to the use of different analytical techniques.

PM10 mass concentrations were included in the model with uncertainties set at four times their values (Kim et al., 2003). In the end, 22 low time resolution variables (PM10 mass, Na, Mg, Al, Si, S, K, Ca, Cr, Mn, Fe, Cu, Zn, Pb, EC, OC, levoglucosan, NO_3^-, b_{ap} 405nm, b_{ap} 532nm, b_{ap} 635nm, b_{ap} 780nm) and 17 hourly variables (Na, Mg, Al, Si, S, K, Ca, Cr, Mn, Fe, Cu, Zn, Pb, b_{ap} 405nm, b_{ap} 532nm, b_{ap} 635nm, b_{ap} 780nm) were considered.

Finally, the input matrix consisted in 386 samples and the total number of time units was 1117. The analysis was performed in the robust mode; lower limit for G contribution was set to -0.2 (Brown et al., 2015) and the error model em=-14 was used for the main equation with C_1= input error, C_2= 0.0 and C_3=0.1 (Paatero, 2012).

To the authors' knowledge, this is the first time that b_{ap} at different wavelengths has been introduced in the multi-time model and used to more robustly identify the sources; moreover, the optical information has been also exploited to retrieve additional information such as the Absorption Ångström Exponent (α) of the sources and MAC values in an original way.

3. Results and discussion

3.1 Source apportionment with multi-time model

Different number of factors (5-10) were explored; after 30 convergent runs, an 8-factor base-case solution corresponding to the lowest Q value (2086.88) was firstly selected (see Fig. S1 in the Supplement). It is important to notice that the model was run using all variables (chemical + optical) as explained in Sect. 2.5. A lower or higher number of factors caused ambiguous chemical profiles as the physical interpretation highlighted clearly mixed sources for a lower number of factors or unique factors in case of more factors (i.e. Pb for 9 factors); moreover, inconsistent mass closure was detected increasing the number of factors (e.g. the sum of species contribution was up to 25 % higher than the mass for the 10-factor solution). In the 8-factor base case solution, the mass was well reconstructed by the model (R^2=0.98), with a slope of 0.98 ± 0.02 and negligible intercept=0.51 ± 0.89 μg m^{-3}.

The factor-to-source assignment process was based on both the Explained Variation (EV) values - which are typically higher for chemical tracers (Lee et al., 1999; Paatero, 2010) - and the physical consistence of factor chemical profiles. In chosen solution, the not explained variation was lower than 0.25 for all variables. The scaled residuals showed a random distribution of negative and positive values in the ± 3 range.

Using EV and chemical profiles reported in Fig. S1 (a), the 8 factors were tentatively assigned to specific atmospheric aerosol sources: nitrate, sulphate, resuspended dust, biomass burning, construction works, traffic, industry, and aged sea salt. In Table S1 (in the Supplement) absolute and relative average source contributions to PM10 mass are reported.

Although the above mentioned base-case solution was a satisfactory representation of the main sources active in the area (as reported in previous works, see e.g. Marcazzan et al., 2003; Vecchi et al., 2009 and 2018; Bernardoni et al., 2011 and 2017a; Amato et al., 2016), the chemical profiles of some factors could be improved exploring rotated solutions. The most relevant case was represented by aged sea-salt where typical diagnostic ratios such as Mg/Na and Ca/Na were not well reproduced (in bulk sea water equal to 0.12 and 0.04, respectively, as reported e.g. in Seinfeld and Pandis, 2006) and the chemical profile itself was too much impacted by the presence of Fe compared to bulk sea water composition. Therefore, the above-mentioned diagnostic ratios were here used as constraints and Fe was maximally pulled down in the chemical profile. The effective increase in Q was of about 61 units (Q=2147), with a percentage increase of about 3 %; as a rule of thumb, an increase in the Q value of a few tens is generally acceptable (Paatero and Hopke, 2009). It is noteworthy that an improvement in the chemical profiles was achieved with negligible differences– compared to the base-case solution – as for all other relevant features of the solution (i.e. EV, residuals, mass reconstruction, source apportionment). Therefore, an 8-factor constrained solution was considered the most physically reliable; results are presented in Table 1 and Fig. 1 and discussed in detail in the following.

Atmos. Chem. Phys. Discuss., https://doi.org/10.5194/acp-2019-123
Manuscript under review for journal Atmos. Chem. Phys.
Discussion started: 12 March 2019

Atmospheric Chemistry and Physics Discussions

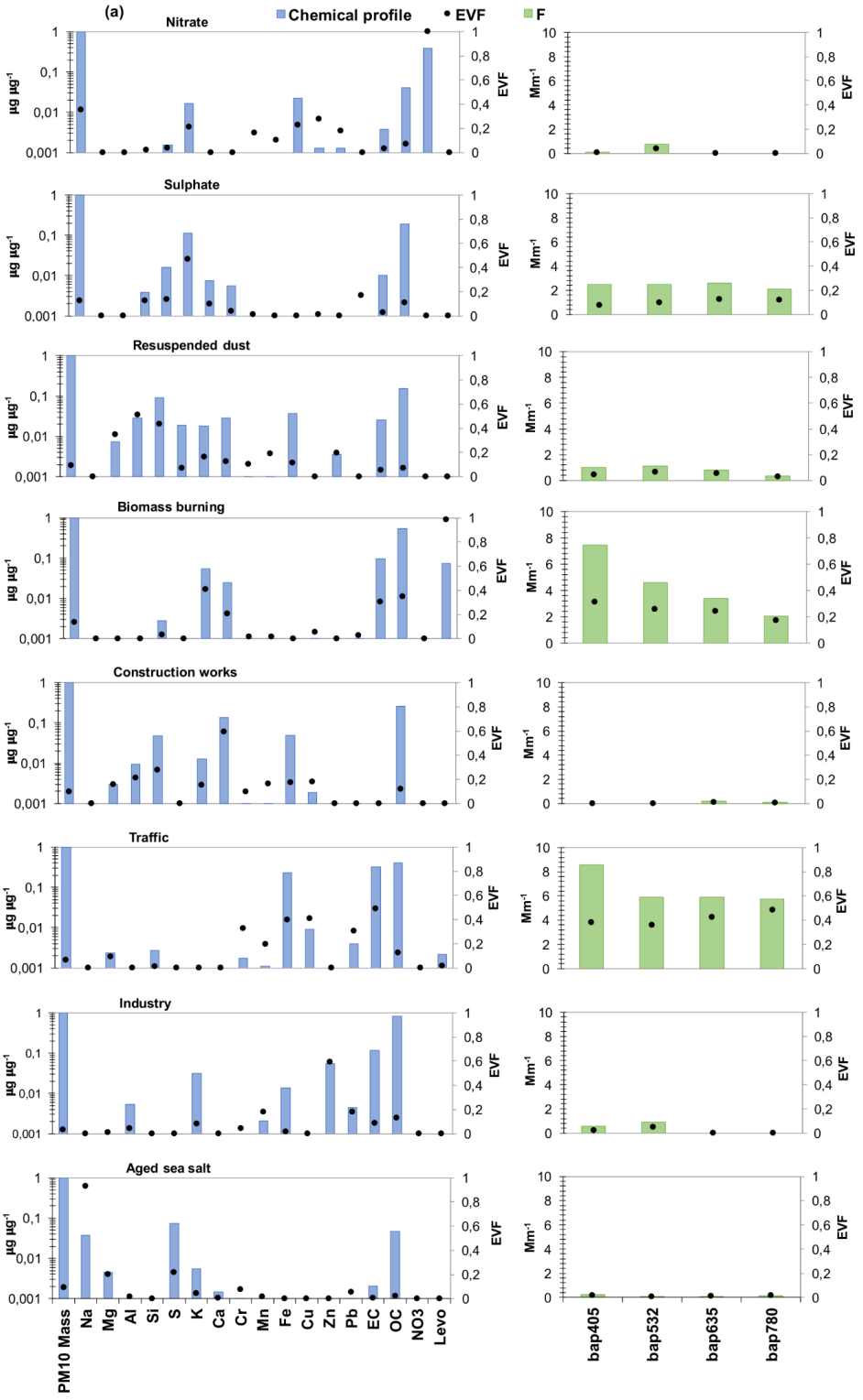

Figure 1: (a) Chemical profiles of the 8-factor constrained solution (b) b_{ap} apportionment of the 8-factor constrained solution.

Factors	Summer [μg m^{-3}]	Winter [μg m^{-3}]	Total [μg m^{-3}]
Nitrate	3.6 (15 %)	21.1 (44 %)	10.2 (31 %)
Sulphate	6.3 (26 %)	8.1 (17 %)	7.0 (21 %)
Re-suspended dust	4.6 (19 %)	1.7 (4 %)	3.5 (11 %)
Biomass burning	0.32 (1 %)	8.3 (17 %)	3.3 (10 %)
Construction works	5.9 (24 %)	3.4 (7 %)	4.9 (15 %)
Traffic	1.4 (6 %)	2.2 (5 %)	1.7 (5 %)
Industry	0.86 (4 %)	1.2 (3 %)	1.0 (3 %)
Aged sea salt	1.4 (6 %)	1.8 (4 %)	1.6 (5 %)

Table 1: Absolute and relative average source contributions to PM10 mass in the 8-factor constrained solution.

In the factor interpreted as nitrate the explained variation is fully ascribed to NO_3^-. This factor contains a significant fraction of nitrate in the chemical profile (39 %) and all nitrate is accounted for only in this factor. This source is by large the most significant source at the investigated site, accounting for about 31 % over the whole campaign (a similar estimate – 26 % - was reported by Amato et al. (2016) during the AIRUSE campaign in Milan in 2013) raising up to 44 % during wintertime (comparable to 37 % reported by Vecchi et al. (2018)). Indeed, the Po valley is well-known for experiencing very high nitrate concentrations during wintertime (Vecchi et al., 2018; and references therein) because of large emissions of gaseous precursors related to urban and industrial activities, wood burning used for residential heating, high ammonia levels due to agricultural fields manure and – last but not the least – poor atmospheric dispersion conditions.

The factor associated to sulphate shows EV=0.47 for S, which contributes to the chemical profile for about 11 % (corresponding to 33 % as SO_4^{2-} and 45 % as ammonium sulphate). Due to the secondary origin of the aerosol associated to this factor, it is not surprising to find also a significant OC contribution (19 %); indeed, as already pointed out for the same location by Vecchi et al. (2018), in Milan aerosol is impacted by highly oxygenated components due to aging processes favoured by strong atmospheric stability (Vecchi et al., 2019). This factor accounts for 21 % of the PM10 mass. It is noteworthy that, on average, factors associated to secondary compounds (i.e. nitrate and sulphate) together account for 52 % of the PM10 mass in the Milan atmosphere for the period under investigation.

The factor identified as re-suspended dust is mainly characterised by high EVs and contributions coming from Al, Si and Mg, i.e. crustal elements. The Al/Si ratio is 0.31, very similar to the literature value for average crust composition (Mason, 1966); the relatively high contribution of OC in the chemical profile (15 %) and the presence of EC (about 2.6 %), indicate that there is very likely a mixing with road dust (Thorpe and Harrison, 2008). This source accounts for about 11 % of the PM10 mass.

The factor identified as biomass burning is characterised by high EV for levoglucosan (0.98), a known tracer for this source as it is generated by cellulose pyrolysis; EV higher than 0.3 are also found for K, OC, and EC. In the source chemical profile, OC contributes for 54 %, EC for 10 %, levoglucosan for 7 %, and K for 5 %. The average biomass burning contribution during this campaign is 10 % (up to 17 % in wintertime). Anticipating the discussion presented in detail in Sect. 3.2, it is worth noticing that in this factor there is also the second largest contribution to the aerosol absorption coefficient after traffic.

The factor presenting a high (0.60) EV for Ca is associated to construction works, following literature works (e.g. Vecchi et al., 2009; Bernardoni et al., 2011; Dall'Osto, 2013; Crilley et al., 2017; Bernardoni et al., 2017a; and references therein). Major contributors to the chemical profile are Ca (13 %), OC (26 %), Fe and Si (5 % each). This factor accounts on average for 15 % to PM10. As already mentioned, during the campaign a not negligible contribution from this source could be expected, due to the presence of a construction building site nearby the monitoring location.

In the factor here assigned to traffic (primary contribution), EV larger than 0.3 are found for EC, Cu, Fe, Cr, and Pb. The highest relative contributions in terms of mass in the chemical profile are given by OC (41 %), EC (32 %), Fe (23 %), and Cu (1 %). The OC-to-EC ratio is about 1.3 which is consistent with a primary traffic contribution (Giugliano et al., 2005; Bernardoni et al., 2011). This traffic (primary) contribution over the whole dataset accounts for 5 % of the PM10 mass with a slightly lower absolute contribution in summer (see Table 1). This contribution is comparable to the percentage (7 %) reported by Amato et al. (2016) for exhaust traffic emissions but it is lower than our previous estimates, i.e. 15 % in 2006 in PM10 and 12 % in PM1 recorded in winter 2012, as reported in Bernardoni et al. (2011) and Vecchi et al. (2018), respectively. However, the current estimate seems to be still reasonable when considering the efforts done in latest years to reduce vehicles exhaust particle emissions and the fraction of secondary nitrate to be added to account for the overall traffic impact; indeed, a significant traffic contribution due to nitrate should be accounted for the relevant nitrogen oxides and ammonia emissions from agriculture in the region (INEMAR ARPA-Lombardia, 2018). Unfortunately, the non-linearity of the emission-to-ambient concentration levels relationship and the high uncertainties in emission inventories still prevent a robust estimate of this secondary contribution to total traffic exhaust emissions. In Sect. 3.2, it will be shown that traffic is the largest contributor to aerosol absorption coefficient, a result that reinforces the interpretation of this factor as a traffic emission source.

The industry factor shows high EV for Zn (0.59); the second highest EV is related to Mn (0.13). Previous studies at the same sampling site identified these elements as tracers for industrial emissions (e.g. Vecchi et al., 2018; and references therein). The chemical profile is enriched by heavy metals and, after traffic, it is the profile with the highest share of Cr, Mn, Fe, Cu, Zn, and Pb (explaining about 8 % of the total PM10 mass in the profile). The industry contribution is not very high in the urban area of Milan, accounting for 3 % on average.

Atmos. Chem. Phys. Discuss., https://doi.org/10.5194/acp-2019-123
Manuscript under review for journal Atmos. Chem. Phys.
Discussion started: 12 March 2019

The factor interpreted as aged sea salt has high EV of Na (0.93) and this element is - as a matter of fact - present only in this factor chemical profile. To check the physical consistency of this assignment and considering that Milan is about 120 km away from the nearest sea coast, back-trajectories frequencies were calculated through the NOAA HYSPLIT trajectory model (Draxler and Hess, 1998; Stein et al., 2015; Rolph et al., 2017). Temporal patterns of Cl concentrations (not inserted in the multi-time analysis as being a weak variable) during episodes were exploited to further confirm the factor-to-source association. As an example, a very short event (13/07 h. 16-18) highlighted by the model and representing the highest sea salt contribution during summer is here analysed in further detail. Before and during the sea salt event, air masses showed a clear origin from south-west compatible with Ligurian sea while soon after the event, there was a rapid change of wind direction (Fig. S2, in the Supplement). These hours were characterised by an average high wind speed of 4.8 ± 1.7 m s^{-1} (with a maximum peak of 9.5 m s^{-1}) compared to 1.9 ± 1.0 m s^{-1} average wind speed recorded during the summer campaign. In addition, Cl concentration and aged sea salt pattern show an evident temporal coincidence in peak occurrence during the event (Fig. 2), thus confirming the correctness of the source identification. During this episode, only the Cl coarse fraction increased (Fig. S3, in the Supplement) and reached about 90 % of total PM10 Cl concentration; Cl/Na ratio was 0.38 ± 0.05, consistent with an aging of marine air masses during advection showing the typical Cl depletion due to the interaction between sea salt particles and polluted air masses (Seinfeld and Pandis, 2006).

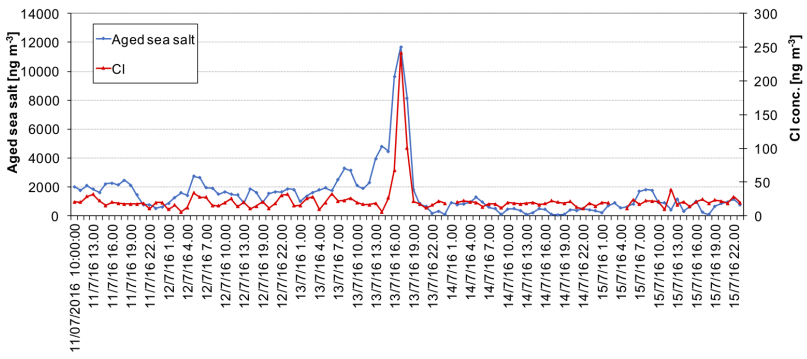

Figure 2: Temporal patterns of aged sea salt source retrieved from the multi-time model and Cl concentrations measured in atmosphere.

Bootstrap analysis was performed to evaluate the uncertainties associated to source profiles (Crespi et al., 2016). 100 runs were carried out (see Fig. 3, values expressed in ng m^{-3} or Mm^{-1} on a logarithmic scale); factors were well mapped, with Pearson coefficient always higher than 0.97, and tracers for each source showed small interquartile range, supporting the goodness of the solution presented in this work.

Atmos. Chem. Phys. Discuss., https://doi.org/10.5194/acp-2019-123
Manuscript under review for journal Atmos. Chem. Phys.
Discussion started: 12 March 2019

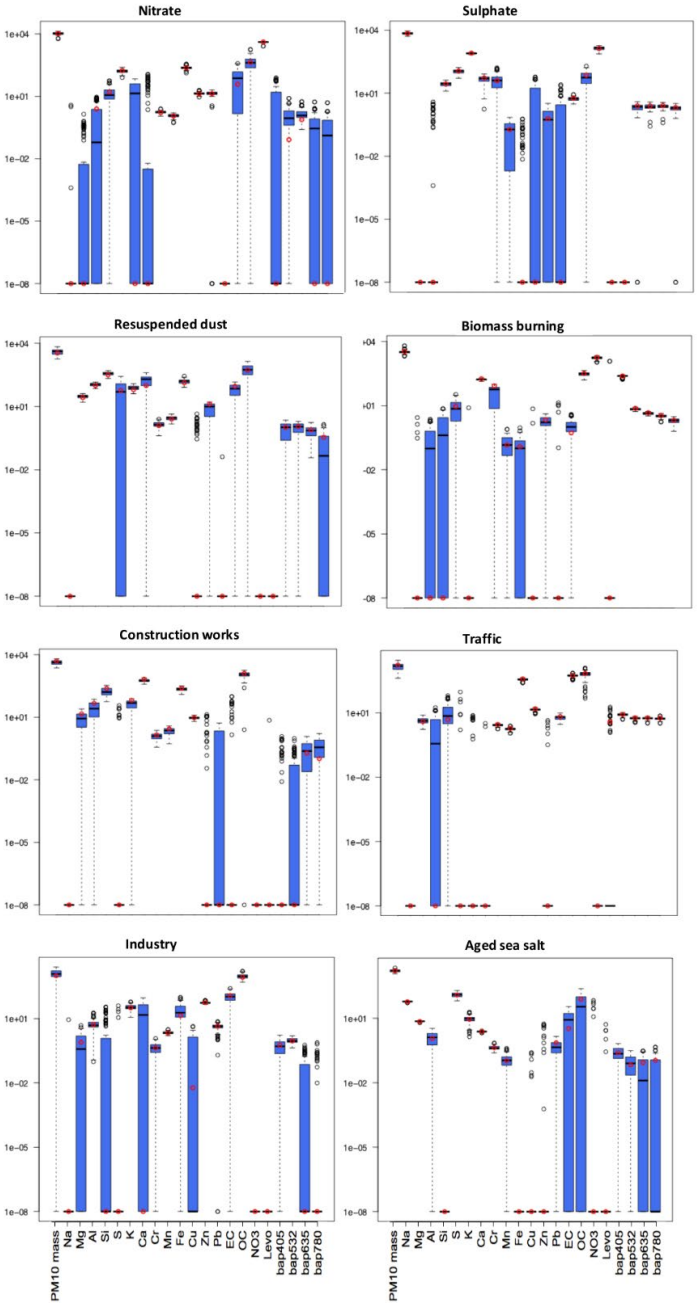

Figure 3: Box plot of the bootstrap analysis on the 8-factor constrained solution. The red dots represent the output values of the solution of the model; the black lines the medians from the bootstrap analysis; the blue bars the 25th and 75th percentile; the dotted lines the interval equal to 1.5 the interquartile range and the black dots the outliers from this interval.

3.2 Improving source apportionment with optical tracers

First of all, the use of the absorption coefficient determined at different wavelengths as input variable in the multi-time model, strengthened the identification of the sources, suggesting that it can be exploited when specific chemical tracers are not available (e.g. levoglucosan for wood burning). To prove that, a separate source apportionment study was performed with EPA PMF 5.0 (Norris et al., 2014), introducing only hourly elemental concentrations from samples collected by the streaker sampler and hourly b_{ap} at different λ measured by PP_UniMI on the same filters. Streaker samples typically lack of a complete chemical characterisation; in particular, important chemical tracers such as levoglucosan and EC are not available. In this analysis, b_{ap} assessed at different wavelengths resulted particularly useful for the identification of the biomass burning factor that explained a significant percentage of the b_{ap} itself (from 25 % to 35 % depending on λ) (Fig. S4, in the Supplement); without this additional information, the factor-to-source assignment would be otherwise based only on the presence of elemental potassium while being well-known that potassium cannot be considered an unambiguous tracer as it is emitted by a variety of sources (see for example Pachon et al., 2013; and references therein).

As for the multi-time model, results showed that the absorption coefficient contribution was higher than 45 % in the factor labelled as traffic, highlighting the importance of exhaust emissions in a factor that would be otherwise characterised mainly on elements related to non-exhaust emissions (Cu, Fe, Cr).

Furthermore, the two factors identified as biomass burning and traffic are the main contributors to aerosol absorption in atmosphere and show significant EV values. Traffic accounts for 55 % of b_{ap} at 780 nm and 42 % at 405 nm; biomass burning accounts for 20 % and 36 % at 780 and 405 nm, respectively. The Explained Variation (EV) of b_{ap} has the maximum value at 405 nm for biomass burning (0.32) and at 780 nm for traffic (0.49), showing the tendency to decrease and increase with the wavelength, respectively. The other six sources are less relevant in terms of EV values and overall contribute for less than 30%.

It is noteworthy that opposite to the approach used in source apportionment optical models, like the widespread Aethalometer model (Sandradewi et al., 2008) and MWAA model (Massabò et al., 2015; Bernardoni et al., 2017b), no a-priori information about the Ångström Absorption Exponent (α) of the fossil fuel and biomass burning sources was introduced in the multi-time model; instead, an estimate for its value can be directly retrieved from the obtained solution. It has to be mentioned that optical models are based on a two-source hypothesis (i.e. biomass burning and fossil fuel emissions). Hereafter, in order to compare multi-time model and optical models results, contributions due to traffic and industry (i.e. emissions most likely connected to fossil fuel usage) were added up and labelled as "fossil fuel emissions".

In Fig. 4 the wavelength dependence of b_{ap} for the biomass burning and the fossil fuel profiles obtained with the multi-time model is shown; the fitting procedure considering $b_{ap} \propto \lambda^{-\alpha}$, gives α_{BB} (α biomass burning) = 1.83 and α_{FF} (α fossil fuels) = 0.80. The bootstrap analysis allowed to estimate the range of variability of α values, considering the 25th and 75th percentile: 0.78-0.88 for α_{FF} and 1.65-1.88 for α_{BB}.

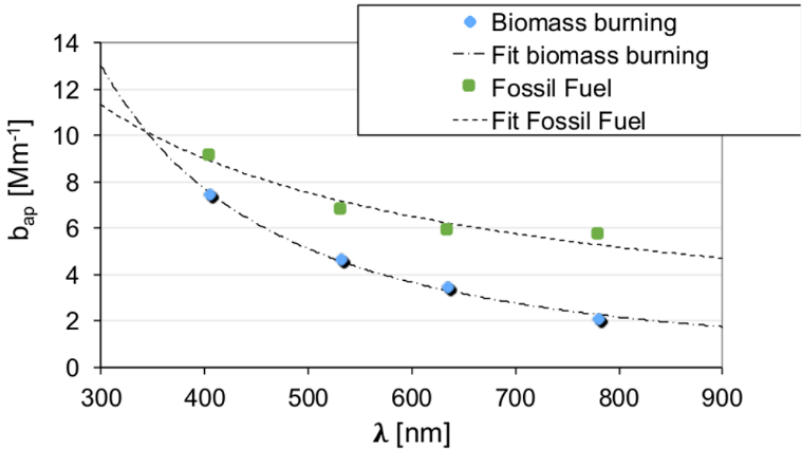

Figure 4: b_{ap} dependence on λ for biomass burning and fossil fuel emissions.

The value of α_{BB} obtained in this work is very similar to 1.86 found for biomass burning by Sandradewi et al. (2008) and 1.8 obtained by Massabò et al. (2015) who used also independent ^{14}C measurements for checking.

The α_{FF} value (assumed to be equal to α_{BC} in source apportionment optical models) obtained in this work is in the range 0.8-1.1 typically reported in optical source apportionment studies (e.g. Bernardoni et al., 2017b; and references therein). It is also consistent with the atmospheric α value obtained during the summer campaign, when biomass burning was negligible (impacting 1 % of the total PM10 mass from the multi-time source apportionment). The assessment of α_{BC} is still an issue and both experimental and simulation studies are in progress to reduce uncertainties and give a better evaluation of this relevant optical parameter; literature works (e.g. Gyawali et al., 2009; Fischer and Smith, 2018; Liu et al. 2018) report α_{BC} values ranging from 0.6 to 1.4 for both coated and bulk particles with a strong dependence from particle size distribution.

Results here reported allow also to study the relationship between the absorption coefficient and the mass of black carbon, i.e. the so called Mass Absorption Cross section (MAC) at different wavelengths. The MAC(λ) =b_{ap}(λ)/BC relationship assumes that black carbon (BC) is the only light-absorbing species present; however, this assumption is not always valid, since mineral dust and brown carbon (BrC) can significantly contribute to aerosol absorption. During our monitoring

campaign, no significant contribution from mineral dust was observed; opposite, biomass burning was proved to be a relevant source so that BrC was certainly a significant contributor (Fuzzi et al., 2015) as also suggested by α_{BB} = 1.83 in the biomass burning factor. The possible overestimation of BC when total b_{ap} is ascribed to BC only is usually minimised choosing a wavelength higher than 600 nm, exploiting the spectral dependence of absorption from different aerosol compounds (Petzold et al., 2013).

EC concentration retrieved from the chemical profiles (see Fig. 1) was used as a proxy for BC to estimate source-dependent $b_{ap}(\lambda)$-to-BC ratio. Results are represented in Fig. 5. It is noteworthy that here this ratio is intentionally not indicated as MAC, since overestimation of the BC absorption especially at lower λ might occur (see previous discussion). BrC is expected to give a small contribution in the fossil fuel source; therefore, the best approximation for MAC(λ) values are likely the $b_{ap}(\lambda)$-to-BC ratios observed in the fossil fuel source at our monitoring site. They resulted to be 13.7 m^2 g^{-1} at λ = 405 nm; 10.2 m^2 g^{-1} at λ = 532 nm; 8.8 m^2 g^{-1} at λ = 635 nm; 8.6 m^2 g^{-1} at λ = 780 nm. At λ = 550 nm Bond and Bergstrom (2006) report MAC = 7.5 ± 1.2 m^2 g^{-1} for uncoated fresh emitted particles and MAC values in polluted regions ranging from 9 to 12 m^2 g^{-1}, attributable to absorption enhancement due to particles coating. The MAC estimate obtained in this work from multi-time model at 532 nm is comparable to literature values and it confirms the importance of aging processes in atmosphere on the optical properties of particles.

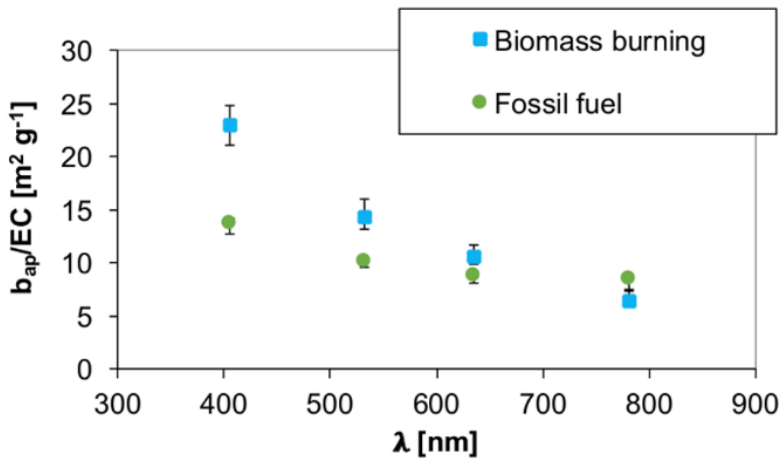

Figure 5: b_{ap}-to-EC ratio dependence on λ for biomass burning and fossil fuel emissions. Error bars represent the 25th and 75th percentile retrieved from the bootstrap analysis.

Ratios in Figure 5 are clearly less comparable at λ=405 nm (see also table 2S); this result is explained by the significant contribution of BrC to b_{ap} at this wavelength in the biomass burning factor.

No seasonal differences in the atmospheric ratios were observed but at λ = 405 nm (see table S2, in the Supplement), for which winter values are higher than summer ones (17.8 ± 0.4 and 14.2 ± 0.5, respectively); this result can be explained considering the influence of biomass burning emissions on BrC concentration in atmosphere during the winter season. From the outputs of the modelling approach here proposed, the apportionment of the biomass burning and fossil fuel contributions to b_{ap} at different wavelengths was also obtained. As expected, the relative contribution to the total reconstructed b_{ap} ascribed to the biomass burning factor decreases with increasing λ, opposite to the contribution from fossil fuel combustion which gives the highest contribution at 780 nm (table 1); in addition, the latter contribution prevails at all wavelengths at the investigated site.

	λ = 405 nm	**λ = 532 nm**	**λ = 635 nm**	**λ = 780 nm**
Biomass burning	36 % (31 %-36 %)	29 % (25 %-30 %)	26 % (23 %-27 %)	20 % (16 %-22 %)
Fossil fuels	45 % (41 %-46 %)	43 % (39 %-44 %)	45 % (41 %-47 %)	55 % (48 %-55 %)

Table 2: Average contribution to total reconstructed b_{ap} for the biomass burning and fossil fuel factors; in parenthesis 25th and 75th percentile are reported.

4. Conclusions

The multi-time model implemented through Multilinear Engine (ME2) script allowed the analysis of experimental data collected at different time scales, coupling the detailed chemical speciation at low time resolution and the temporal information given by high time resolution samples. The effect of the introduction of the aerosol absorption coefficient (b_{ap}) measured at different wavelengths in the modelling process was investigated and gave promising results. First of all, a more robust identification of sources was provided; secondly, it paved the way to the retrieval of optical apportionment and optical characterisation of the sources (e.g. estimate of source-specific Ångström Absorption Exponent - α - and MAC at different wavelengths). It is worthy to note that – at the state of the art – in source apportionment optical models (e.g. Aethalometer model) values for α related to fossil fuel emissions and wood burning are fixed by the modeller thus carrying a large part of the uncertainties in the model results. The original approach described in this work can be applied to any source apportionment study using any suitable dataset (not necessarily with multi-time resolution). Besides the traditional source apportionment, the impact of different sources on the aerosol absorption coefficient was estimated; this piece of information can be very useful to formulate strategies of pollutants abatement, in order to improve air quality and to face climate challenges. In particular, at the investigated site secondary compounds constituted the highest contribution in terms of PM10 mass (52 % on average), while the two factors identified as biomass burning and traffic

were found to be the most significant contributors to aerosol absorption in atmosphere, in agreement with available literature works.

Acknowledgements

This work was partially funded by the Italian National Institute of Nuclear Physics under the INFN experiments DEPOTMASS and TRACCIA. ACTRIS-IT funded the publication of the paper. The authors thank Prof. Paola Fermo (Dept. of Chemistry, University of Milan) for availability of the Sunset instrument to perform EC/OC analyses. The mechanical workshop of the Dept. of Physics – University of Milan is gratefully acknowledged for the realisation of parts of the polar photometer. The authors acknowledge also ARPA – Lombardia for meteorological data availability.

Data availability.

The data in the study are available from the authors upon request (roberta.vecchi@unimi.it).

Supplement.

The supplement related to this article is available online

Author contributions.

ACF performed streaker sampling and related optical analysis, implemented the advanced model, analysed the results, and drafted the paper. GV contributed to model implementation and data reduction. VB, SV, and REP carried out the sampling campaign on filters, performed the optical measurements and data analysis. GC, SN, and FL performed PIXE analysis and data reduction. DM and PP carried out ionic characterisation on filters and data analysis. RV was responsible for the design and coordination of the study, the synthesis of the results and the final version of the paper. All authors contributed to the interpretation of the results obtained with the new approach here described and revised the manuscript content giving a final approval of the version to be submitted.

Competing interests.

The authors declare that they have no conflict of interest.

References

Amato F., Alastuey A., Karanasiou A., Lucarelli F., Nava S., Calzolai G., Severi M., Becagli S., Gianelle V.N., Colombi C., Alves C., Custódio D., Nunes T., Cerqueira M., Pio C., Eleftheriadis K., Diapouli E., Reche C., Minguillón M.C., Manousakas M.I., Maggos T., Vratolis S., Harrison R.M. and Querol X.: AIRUSE-LIFE+: a harmonized PM speciation and source apportionment in five southern European cities, Atmos. Chem. Phys., 16, 3289-3309, https://doi.org/10.5194/acp-16-3289-2016, 2016.

Andreae M.O. and Gelencsér A.: Black carbon or brown carbon? The nature of light-absorbing carbonaceous aerosols, Atmos. Chem. Phys., 6, 3131-3148, https://doi.org/10.5194/acp-6-3131-2006, 2006.

Belis C.A., Larsen B.R., Amato F., El Haddad I., Favez O., Harrison R.M., Hopke P.K., Nava S., Paatero P., Prèvot A., Quass U., Vecchi R. and Viana M.: European Guide on Air Pollution Source Identification with Receptor Models, Luxembourg: Publications Office of the European Union, Joint Research Center – Institute for Environment and Sustainability, European Union, https://doi.org/10.2788/9332, 2014.

Belis C.A., Karagulian F., Amato F., Almeida M., Artaxo P., Beddows D.C.S., Bernardoni V., Bove M.C., Carbone S., Cesari D., Contini D., Cuccia E., Diapouli E., Eleftheriadis K., Favez O., El Haddad I., Harrison R.M., Hellebust S., Hovorka J., Jang E., Jorquera H., Kammermeier T., Karl M., Lucarelli F., Mooibroek D., Nava S., Nøjgaard J.K., Paatero P., Pandolfi M., Perrone M.G., Petit J.E., Pietrodangelo A., Pokorná P., Prati P., Prevot A.S.H., Quass U., Querol X., Saraga D., Sciare J., Sfetsos A., Valli G., Vecchi R., Vestenius M., Yubero E. and Hopke P.K.: A new methodology to assess the performance and uncertainty of source apportionment models II: The results of two European intercomparison exercises, Atmos. Environ., 123, 240-250, https://doi.org/10.1016/j.atmosenv.2015.10.068, 2015.

Bernardoni V., Vecchi R., Valli G., Piazzalunga A. and Fermo P.: PM10 source apportionment in Milan (Italy) using time-resolved data, Sci. Total Environ., 409, 4788-4795, https://doi.org/10.1016/j.scitotenv.2011.07.048, 2011.

Bernardoni V., Elser M., Valli G., Valentini S., Bigi A., Fermo P., Piazzalunga A. and Vecchi R.: Size-segregated aerosol in a hot-spot pollution urban area: Chemical composition and three-way source apportionment, Environ. Pollut., 231, 601-611, https://doi.org/10.1016/j.envpol.2017.08.040, 2017a.

Bernardoni V., Pileci R.E., Caponi L. and Massabò D.: The Multi-Wavelength Absorption Analyzer (MWAA) model as a tool for source and component apportionment based on aerosol absorption properties: application to samples collected in different environments, Atmosphere, 8, 218, https://doi.org/10.3390/atmos8110218, 2017b.

Bernardoni V., Valli G. and Vecchi R.: Set-up of a multi-wavelength polar photometer for the off-line measurement of light absorption properties of atmospheric aerosol collected with high-temporal resolution, J. Aerosol. Sci., 107, 84-93, https://doi.org/10.1016/j.jaerosci.2017.02.009, 2017c.

Bigi A. and Ghermandi G.: Long-term trend and variability of atmospheric PM_{10} concentration in the Po Valley, Atmos. Chem. Phys., 14, 4895-4907, https://doi.org/10.5194/acp-14-4895-2014, 2014.

Bond T.C. and Bergstrom R.W.: Light absorption by carbonaceous particles: an investigative review, Aerosol Sci. Tech., 40, 27-67, https://doi.org/10.1080/02786820500421521, 2006.

Bond T.C., Doherty S.J., Fahey D.W., Forster P.M., Berntsen T., DeAngelo B.J., Flanner M.G., Ghan S., Kärcher B., Koch D., Kinne S., Kondo Y., Quinn P.K., Sarofim M.C., Schultz M.G., Schulz M., Venkataraman C., Zhang H., Zhang S., Bellouin N., Guttikunda S.K., Hopke P.K., Jacobson M.Z., Kaiser J.W., Klimont Z., Lohmann U., Schwarz J.P., Shindell D., Storelvmo T., Warren S.G. and Zender C.S.: Bounding the role of black carbon in the climate system: A scientific assessment, J. Geophys. Res.-Atmos., 118, 5380-5552, https://doi.org/10.1002/jgrd.50171, 2013.

Brown S.G., Eberly S., Paatero P. and Norris G.A.: Methods for estimating uncertainty in PMF solutions: Examples with ambient air and water quality data and guidance on reporting PMF results, Sci. Total Environ., 518-519, 626-635, https://doi.org/10.1016/j.scitotenv.2015.01.022, 2015.

Calzolai G., Chiari M., Lucarelli F., Mazzei F., Nava S., Prati P., Valli G. and Vecchi R.: PIXE and XRF analysis of particulate matter samples: an inter-laboratory comparison, Nucl. Instrum. Meth. B, 266, 2401-2404, https://doi.org/10.1016/j.nimb.2008.03.056, 2008.

Calzolai G., Lucarelli F., Chiari M., Nava S., Giannoni M., Carraresi L., Prati P. and Vecchi R.: Improvements in PIXE analysis of hourly particulate matter samples, Nucl. Instrum. Meth. B, 363, 99-104, https://doi.org/10.1016/j.nimb.2015.08.022, 2015.

Crespi A., Bernardoni V., Calzolai G., Lucarelli F., Nava S., Valli G. and Vecchi R.: Implementing constrained multi-time approach with bootstrap analysis in ME-2: an application to PM2.5 data from Florence (Italy), Sci. Total Environ., 541, 502-511, https://doi.org/10.1016/j.scitotenv.2015.08.159, 2016.

Crilley L.R., Lucarelli F., Bloss W.J., Harrison R.M., Beddows D.C., Calzolai G., Nava S., Valli G., Bernardoni V. and Vecchi R.: Source Apportionment of Fine and Coarse Particles at a Roadside and Urban Background Site in London during the Summer ClearfLo Campaign, Environ. Pollut., 220, 766-778, https://doi.org/10.1016/j.envpol.2016.06.002, 2017.

D'Alessandro A., Lucarelli F., Mandò P.A., Marcazzan G., Nava S., Prati P., Valli G., Vecchi R. and Zucchiatti A.: Hourly elemental composition and sources identification of fine and coarse PM10 particulate matter in four Italian towns, J. Aerosol Sci., 34, 243-259, https://doi.org/10.1016/S0021-8502(02)00172-6, 2003.

Dall'Osto, M., Querol, X., Amato, F., Karanasiou, A., Lucarelli, F., Nava, S., Calzolai, G. and Chiari, M.: Hourly elemental concentrations in PM2.5 aerosols sampled simultaneously at urban background and road site during SAPUSS e diurnal variations and PMF receptor modelling, Atmos. Chem. Phys., 13, 4375-4392, https://doi.org/10.5194/acp-13-4375-2013, 2013.

Draxler R.R. and Hess G.D.: An overview of the HYSPLIT_4 modelling system for trajectories, dispersion, and deposition, Aust. Meteorol. Mag., 47, 295-308, 1998.

Fialho P., Hansen A.D.A. and Honrath R.E.: Absorption coefficients by aerosols in remote areas: a new approach to decouple dust and black carbon absorption coefficients using seven-wavelength Aethalometer data, J. Aerosol Sci., 36, 267-282, https://doi.org/10.1016/j.jaerosci.2004.09.004, 2005.

Fischer D.A. and Smith G.D.: A portable, four wavelength, single-cell photoacoustic spectrometer for ambient aerosol absorption, Aerosol Sci. Tech., 52, 393-406, https://doi.org/10.1080/02786826.2017.1413231, 2018.

Fuzzi S., Baltensperger U., Carslaw K., Decesari S., Denier van der Gon H., Facchini M.C., Fowler D., Koren I., Langford B., Lohmann U., Nemitz E., Pandis S., Riipinen I., Rudich Y., Schaap M., Slowik J.G., Spracklen D.V., Vignati E., Wild M., Williams M. and Gilardoni S.: Particulate matter, air quality and climate: lessons learned and future needs, Atmos. Chem. Phys, 15, 8217-8299, https://doi.org/10.5194/acp-15-8217-2015, 2015.

Giugliano M., Lonati G., Butelli P., Romele L., Tardivo R. and Grosso M.: Fine particulate (PM2.5-PM1) at urban sites with different traffic exposure, Atmos. Environ., 39, 2421-2431, https://doi.org/10.1016/j.atmosenv.2004.06.050, 2005.

Gyawali M., Arnott W.P., Lewis K. and Moosmüller H.: In situ aerosol optics in Reno, NV, USA during and after the summer 2008 California wildfires and the influence of absorbing and non-absorbing organic coatings on spectral light absorption, Atmos.Chem.Phys, 9, 8007-8015, https://doi.org/10.5194/acp-9-8007-2009, 2009.

Hennigan C.J., Sullivan A.P., Collett J.L.Jr and Robinson A.L.: Levoglucosan stability in biomass burning particles exposed to hydroxyl radicals, Geophys. Res. Lett., 37, 9, https://doi.org/10.1029/2010GL043088, 2010.

Henry R.C.: History and fundamentals of multivariate air quality receptor models, Chemometr. Intell. Lab., 37, 37-42, https://doi.org/10.1016/S0169-7439(96)00048-2, 1997.

Hopke P.K.: Review of receptor modeling methods for source apportionment, J. Air Waste Manage., 66, 3, 237-259, https://doi.org/10.1080/10962247.2016.1140693, 2016.

INEMAR - ARPA Lombardia: INEMAR, Inventario Emissioni in Atmosfera: emissioni in Regione Lombardia nell'anno 2014 - dati finali, ARPA Lombardia Settore Monitoraggi Ambientali, http://www.inemar.eu/xwiki/bin/view/Inemar/HomeLombardia, 2018.

IPCC: Climate Change 2013: The Physical Science Basis. Contribution of Working Group I to the Fifth Assessment Report of the Intergovernmental Panel on Climate Changes, Stocker T.F., Qin D., Plattner G.-K., Tignor M., Allen S.K., Boschung J., Nauels A., Xia Y., Bex V. and P.M. Midgley, Cambridge University Press, Cambridge, United Kingdom and New York, NY, USA, https://doi.org/10.1017/CBO9781107415324, 2013.

Kim E., Hopke P.K. and Edgerton E.S.: Source identification of Atlanta aerosol by positive matrix factorization, J. Air Waste Manage., 53, 6, 731-739, https://doi.org/10.1080/10473289.2003.10466209, 2003.

Kuo C.-P., Liao H.-T., Chou C.C.-K. and Wu C.-F.: Source apportionment of particulate matter and selected volatile organic compounds with multiple time resolution data, Sci. Total Environ., 472, 880-887, https://doi.org/10.1016/j.scitotenv.2013.11.114, 2014.

Lee E., Chan C.K. and Paatero P.: Application of positive matrix factorization in source apportionment of particulate pollutants in Hong Kong, Atmos. Environ., 33, 3201-3212, https://doi.org/10.1016/S1352-2310(99)00113-2, 1999.

Liao H.-T., Chou C.C.-K., Chow J.C., Watson J.G., Hopke P.K. and Wu C.-F.: Source and risk apportionment of selected VOCs and $PM_{2.5}$ species using partially constrained receptor models with multiple time resolution data, Environ. Pollut., 205, 121-130, https://doi.org/10.1016/j.envpol.2015.05.035, 2015.

Liu C., Chung C.E., Yin Y. and Schnaiter M.: The absorption Ångström exponent of black carbon: from numerical

aspects. Atmos. Chem. Phys., 18, 6259-6273, https://doi.org/10.5194/acp-2017-836, 2018.

Marcazzan G.M., Ceriani M., Valli G. and Vecchi R.: Source apportionment of PM10 and PM2.5 in Milan (Italy) using receptor modelling, Sci. Total Environ., 317, 137-147, https://doi.org/10.1016/S0048-9697(03)00368-1, 2003.

Mason B.: Principles of geochemistry, 3rd Edition, John Wiley & Sons, New York, 1966.

Massabò D., Caponi L., Bernardoni V., Bove M.C., Brotto P., Calzolai G., Cassola F., Chiari M., Fedi M.E., Fermo P., Giannoni M., Lucarelli F., Nava S., Piazzalunga A., Valli G., Vecchi R. and Prati P.: Multi-wavelength optical determination of black and brown carbon in atmospheric aerosols, Atmos. Environ., 108, 1-12, https://doi.org/10.1016/j.atmosenv.2015.02.058, 2015.

Massabò D., Caponi L., Bove M.C. and Prati P.: Brown carbon and thermal-optical analysis: A correction based on optical multi-wavelength apportionment of atmospheric aerosols, Atmos. Environ., 125, 119-125, https://doi.org/10.1016/j.atmosenv.2015.11.011, 2016.

Norris G., Duvall R., Brown S. and Bai S.: EPA Positive Matrix Factorization (PMF) 5.0. Fundamentals and User Guide, U.S. Environmental Protection Agency, Washington, DC, 2014.

Ogulei D., Hopke P.K., Zhou L., Paatero P., Park S.S. and Ondov J.M.: Receptor modeling for multiple time resolved species: the Baltimore supersite, Atmos. Environ., 39, 3751-3762, https://doi.org/10.1016/j.atmosenv.2005.03.012, 2005.

Paatero P.: Least squares formulation of robust non-negative factor analysis, Chemometr. Intell. Lab., 37, 23-35, https://doi.org/10.1016/S0169-7439(96)00044-5, 1997.

Paatero P.: The Multilinear Engine – A Table-drive least squares program for solving multilinear problems, including the n-way parallel factor analysis model, J. Comput. Graph. Stat., 8, 4, 854-888, https://doi.org/10.1080/10618600.1999.10474853, 1999.

Paatero P.: User's guide for the Multilinear Engine program "ME2" for fitting multilinear and quasi-multilinear models, University of Helsinki, Department of Physics, Finland, 2000.

Paatero P.: User's Guide for Positive Matrix Factorization programs PMF2 and PMF3, Part 2: reference, available www.helsinki.fi/~paatero/PMF/pmf2.zip (PMFDOC2.pdf), last update 2010.

Paatero P.: The Multilinear Engine (ME-2) script language (v. 1.352), available with the program ME-2 (me2scrip.txt). 2012.

Paatero P.: User's guide for positive matrix factorization programs PMF2 and PMF3, part 1: Tutorial, available at www.helsinki.fi/~paatero/PMF/pmf2.zip (PMFDOC1.pdf), last update 2015.

Paatero P. and Hopke P.K.: Rotational tools for factor analytic models. J. Chemometr., 23, 91-100, https://doi.org/10.1002/cem.1197, 2009.

Paatero P. and Tapper U.: Positive Matrix Factorization: a non-negative factor model with optimal utilization of error estimates of data values, Environmetrics, 5, 111-126, https://doi.org/10.1002/env.3170050203, 1994.

Pachon J.E., Weber R.J., Zhang X., Mulholland J.A. and Russell A.G.: Revising the use of potassium (K) in the source apportionment of PM2.5, Atmos. Pollut. Res., 4, 14-21, https://doi.org/10.5094/APR.2013.002, 2013.

Perrino C., Catrambone M., Dalla Torre S., Rantica E., Sargolini T. and Canepari S.: Seasonal variations in the chemical composition of particulate matter: a case study in the Po Valley. Part I: macro-components and mass closure, Environ. Sci. Pollut. Res., 21, 3999-4009, https://doi.org/10.1007/s11356-013-2067-1, 2014.

Perrone M.G., Larsen B.R., Ferrero L., Sangiorgi G., De Gennaro G., Udisti R., Zangrando R., Gambaro A. and Bolzacchini E.: Sources of high PM2.5 concentrations in Milan, Northern Italy: Molecular marker data and CMB modelling. Sci. Total Environ., 414, 343-355, https://doi.org/10.1016/j.scitotenv.2011.11.026, 2012.

Petzold A., Ogre J.A., Fiebig M., Laj P., Li S.-M., Baltensperger U., Holzer-Popp T., Kinne S., Pappalardo G., Sugimoto N., Wehrli C., Wiedensohler A. and Zhang X.-Y.: Recommendations for the interpretation of "black carbon"

measurements, Atmos. Chem. Phys., 13, 8365-8379, https://doi.org/10.5194/acp-13-8365-2013, 2013.

Piazzalunga A., Fermo P., Bernardoni V., Vecchi R., Valli G. and De Gregorio M.A.: A simplified method for levoglucosan quantification in wintertime atmospheric particulate matter by high performance anion-exchange chromatography coupled with pulsed amperometric detection, Int. J. Environ. Anal. Chem., 90, 934–947, https://doi.org/10.1080/03067310903023619, 2010.

Piazzalunga A., Bernardoni V., Fermo P., Valli G. and Vecchi R. Technical note: On the effect of water-soluble compounds removal on EC quantification by TOT analysis in urban aerosol samples, Atmos. Chem. Phys., 11, 10193–10203, https://doi.org/10.5194/acp-11-10193-2011, 2011.

Piazzalunga A., Bernardoni V., Fermo P. and Vecchi R.: Optimisation of analytical procedures for the quantification of ionic and carbonaceous fractions in the atmospheric aerosol and application to ambient samples, Anal. Bioanal. Chem., 405, 1123-1132, https://doi.org/10.1007/s00216-012-6433-5, 2013.

Polissar A., Hopke P.K., Paatero P., Malm W.C. and Sisler J.F.: Atmospheric aerosol over Alaska: elemental composition and sources. J. Geophys. Res. 103, 19045-19057, https://doi.org/10.1029/98JD01212, 1998.

Pope III C.A. and Dockery D.W.: Health effects of fine particulate air pollution: lines that connect, J. Air Waste Manage., 56, 709-742, https://doi.org/10.1080/10473289.2006.10464485, 2006.

Robinson A.L., Donahue N.M. and Rogge W.F.: Photochemical oxidation and changes in molecular composition of organic aerosol in the regional context, J. Geophys. Res., 111, D3, https://doi.org/10.1029/2005JD006265, 2006.

Rolph G., Stein A. and Stunder B.: Real-time Environmental Application and Display sYstem: READY, Environ. Modell. Softw., 95, 210-228, https://doi.org/10.1016/j.envsoft.2017.06.025, 2017.

Sandradewi J., Prévôt A.S.H., Szidat S., Perron N., Alfarra M.R., Lanz V.A., Weingartner E. and Balternsperger U.: Using aerosol light absorption measurements for the quantitative determination of wood burning and traffic emission contributions to particulate matter, Environ. Sci. Technol., 42, 3316-3323, 2008.

Seinfeld J.H. and Pandis S.N.: Atmospheric chemistry and physics: from air pollution to climate change, 2nd edition, John Wiley & Sons, INC, Hoboken, New Jersey, 2006.

Sofowote U.M., Healy R.M., Su Y., Debosz J., Noble M., Munoz A., Jeong C.-H., Wang J.M., Hilker N., Evans G.J. and Hopke P.K.: Understanding the $PM_{2.5}$ imbalance between a far and near-road location: Results of high temporal frequency source apportionment and parameterization of black carbon, Atmos. Environ., 173, 277-288, https://doi.org/10.1016/j.atmosenv.2017.10.063, 2018.

Stein A.F., Draxler R.R., Rolph G.D., Stunder B.J.B., Cohen M.D. and Ngan F.: NOAA's Hysplit atmospheric transport and dispersion modeling system, Bull. Am. Meteorol. Soc., 96, 2059-2077, https://doi.org/10.1175/BAMS-D-14-00110.1, 2015.

Thorpe A. and Harrison R.M.: Sources and properties of non-exhaust particulate matter from road traffic: A review, Sci. Total Environ., 400, 270-282, https://doi.org/10.1016/j.scitotenv.2008.06.007, 2008.

Vecchi R., Marcazzan G., Valli G., Ceriani M. and Antoniazzi C.: The role of atmospheric dispersion in the seasonal variation of PM1 and PM2.5 concentration and composition in the urban area of Milan (Italy), Atmos. Environ., 38, 4437–4446, https://doi.org/10.1016/j.atmosenv.2004.05.029, 2004.

Vecchi R., Marcazzan G. and Valli G.: A study on nighttime-daytime PM10 concentration and elemental composition in relation to atmospheric dispersion in the urban area of Milan (Italy), Atmos. Environ., 41, 2136-2144, https://doi.org/10.1016/j.atmosenv.2006.10.069, 2007.

Vecchi R., Bernardoni V., Fermo P., Lucarelli F., Mazzei F., Nava S., Prati P., Piazzalunga A. and Valli G.: 4-hours resolution data to study PM10 in a "hot spot" area in Europe, Environ. Monit. Assess., 154, 283–300, https://doi.org/10.1007/s10661-008-0396-1, 2009.

Vecchi R., Bernardoni V., Paganelli C. and Valli G.: A filter-based light absorption measurement with polar photometer: effects of sampling artefacts from organic carbon, J. Aerosol. Sci., 70, 15-25,

https://doi.org/10.1016/j.jaerosci.2013.12.012, 2014.

Vecchi R., Bernardoni V., Valentini S., Piazzalunga A., Fermo P. and Valli G.: Assessment of light extinction at a European polluted urban area during wintertime: Impact of PM1 composition and sources, Environ. Pollut., 233, 679-689, https://doi.org/10.1016/j.envpol.2017.10.059, 2018.

Vecchi R., Piziali F.A., Valli G., Favaron M. and Bernardoni V.: Radon-based estimates of equivalent mixing layer heights: A long-term assessment, Atmos. Environ., 197, 150-158, https://doi.org/10.1016/j.atmosenv.2018.10.020, 2019.

Wang Y., Hopke P.K., Rattigan O.V., Xia X., Chalupa D.C. and Utell M.J.: Characterization of residential wood combustion particles using the two-wavelenght aethalometer, Environ. Sci. Technol., 45, 7387-7393, https://doi.org/10.1021/es2013984, 2011.

Wang Y., Hopke P.K., Rattigan O.V., Chalupa D.C. and Utell M.J.: Multiple-year black carbon measurements and source apportionment using Delta-C in Rochester, New York, J. Air Waste Manage., 62, 8, 880-887, https://doi.org/10.1080/10962247.2012.671792, 2012.

Watson J.G.: Visibility: Science and Regulation, J. Air Waste Manage., 52, 628-713, https://doi.org/10.1080/10473289.2002.10470813, 2002.

Xie M., Chen X., Holder A.L., Hays M.D., Lewandowski M., Offenberg J.H., Kleindienst T.E., Jaoui M. and Hannigan M.P.: Light absorption of organic carbon and its sources at a southeastern U.S. location in summer, Environ. Pollut., 244, 38-46, https://doi.org/10.1016/j.envpol.2018.09.125, 2019.

Yang M., Howell S.G., Zhuang J. and Huebert B.J.: Attribution of aerosol light absorption to black carbon, brown carbon, and dust in China – interpretations of atmospheric measurements during EAST-AIRE, Atmos. Chem. Phys., 9, 2035-2050, https://doi.org/10.5194/acp-9-2035-2009, 2009.

Zhou L., Hopke P.K., Paatero P., Ondov J.M., Pancras J.P., Pekney N.J. and Davidson C.I.: Advanced factor analysis for multiple time resolution aerosol composition data, Atmos. Environ., 38, 4909-4920, https://doi.org/10.1016/j.atmosenv.2004.05.040, 2004.

Zotter P., Herich H., Gysel M., El-Haddad I., Zhang Y., Mocnik G., Hüglin C., Baltensperger U., Szidat S. and Prévôt A.S.H.: Evaluaton of the absorption Ångström exponents for traffic and wood burning in the Aethalometer-based source apportionment using radiocarbon measurements of ambient aerosol, Atmos. Chem. Phys., 17, 4229-4249, https://doi.org/10.5194/acp-17-4229-2017, 2017.

List of Captions

Figure 1: (a) Chemical profiles of the 8-factor constrained solution (b) bap apportionment of the 8-factor constrained solution.

Figure 2: Temporal patterns of aged sea salt source retrieved from the multi-time model and Cl concentrations measured in atmosphere.

Figure 3: Box plot of the bootstrap analysis on the 8-factor constrained solution. The red dots represent the output values of the solution of the model; the black lines the medians from the bootstrap analysis; the blue bars the 25th and 75th percentile; the dotted lines the interval equal to 1.5 the interquartile range and the black dots the outliers from this interval.

Figure 4: b_{ap} dependence on λ for biomass burning and fossil fuel emissions.

Figure 5: b_{ap}-to-EC ratios dependence on λ for biomass burning and fossil fuel emissions. Error bars represent the 25th and 75th percentile retrieved from the bootstrap analysis.

Table 1: Absolute and relative average source contributions to PM10 mass in the 8-factor constrained solution.

Table 2: Average contribution to total reconstructed bap for the biomass burning and fossil fuel factors; in parenthesis 25th and 75th percentile are reported.